

# Nanostructured Tetrahedrite Synthesis for Thermoelectric Applications

Stefano Fasolin, Stefania Fiameni\*, Carlo Fanciulli, Simone Battiston, Alessia Famengo, and Monica Fabrizio

*National Research Council of Italy-Institute of Condensed Matter Chemistry and Technologies for Energy, Padova 35127, Lecco 23900, Italy*

Nowadays, a big challenge in the thermoelectric field is the identification of efficient thermoelectric materials but inexpensive, easy to synthesize, and comprised of Earth-abundant elements. On this basis, tetrahedrite mineral family ( $\text{Cu}_{12-x}\text{Tr}_x\text{Sb}_4\text{S}_{13}$  where  $\text{Tr} = \text{Cu, Mn, Fe, Co, Ni, Zn}$ ) seems to be an attractive *p*-Type Pb-free thermoelectric material, showing a relatively high conversion efficiency. In this work, a solvothermal synthesis method was developed for undoped tetrahedrite  $\text{Cu}_{12}\text{Sb}_4\text{S}_{13}$  and the introduction of Zn and Ni as substituents of copper was also tested. The influence of the stoichiometry and the synthesis conditions on the tetrahedrite phase content and density of the samples were investigated by X-ray diffraction (with profile Rietveld refinements) and scanning electron microscope (equipped with energy dispersive X-ray spectroscopy). Preliminary sintering test were performed by Open Die Pressing.

**Keywords:** Solvothermal Synthesis, Nanostructured Tetrahedrite, Thermoelectric.

## 1. INTRODUCTION

A current challenge in the thermoelectric field is the discovery of new materials which are inexpensive, easy to synthesize, and comprised of earth-abundant elements.

Recently natural mineral tetrahedrites received great interest from thermoelectric society because of its non-toxicity, environmental friendliness and relatively high abundance.

The pure  $\text{Cu}_{12}\text{Sb}_4\text{S}_{13}$  composition does not occur in natural minerals. Natural “tetrahedrite” exists as a solid solution of tetrahedrite ( $\text{Cu}_{12}\text{Sb}_4\text{S}_{13}$ ) and tennantite ( $\text{Cu}_{12}\text{As}_4\text{S}_{13}$ ) where the Cu atoms are partially replaced by transition metal elements such as Zn, Fe, Mn, Hg or Ni.<sup>1–3</sup> The tetrahedrite/tennantite mineral family is the most widespread sulfosalt on Earth. These minerals are found as single crystal or as aggregates in hydrothermal veins in Pb–Zn deposits, with a formation temperature between 300 °C and 350 °C. As single crystal they are relatively abundant in USA<sup>4</sup> and Peru<sup>5,6</sup> in many sulphide deposit, where the main mining interest is related to Cu and Ag presence.<sup>7</sup> In Europe the tetrahedrite family minerals rarely occurred as single crystal (in some sulfosalt-rich

hydrothermal veins in Romania<sup>8</sup> and Bulgaria<sup>9</sup>) but more commonly they are present as accessory mineral (up to 1 wt%) in hydrothermal rocks (Sveeden and Sardinia).<sup>10–12</sup>

The tetrahedrite/tennantite minerals are always associated to other sulfosalts such as pyrite, chalcopyrite, sphalerite and this causes many difficulties regarding the possibility to separate the tetrahedrite from the other associated minerals. Moreover, natural tetrahedrites generally contain Hg and As, often in significant percentage (up to 18 wt% Hg).<sup>13</sup>

The ZT values obtained for synthetic tetrahedrite  $\text{Cu}_{12}\text{Sb}_4\text{S}_{13}$  is 0.56 at 673 K.<sup>14</sup> Synthetic tetrahedrites were variously doped, with interesting results for Ni doped samples with a maximum ZT of 0.7 at 665 K for  $\text{Cu}_{10.5}\text{Ni}_{1.5}\text{Sb}_4\text{S}_{13}$ .<sup>15</sup> Zn substituted tetrahedrites  $\text{Cu}_{10}\text{Zn}_x\text{Sb}_4\text{S}_{13}$  achieved a ZT value near the unity for  $x = 1$  and 1.5.<sup>14</sup> Lu et al.<sup>16</sup> reported a ZT above unity for co-doped Ni and Zn tetrahedrite at 723 K.

For all this reasons it is important to develop a synthetic route to obtain environmental friendly tetrahedrite conveniently doped to be used as thermoelectric materials.

All the synthesis reported in thermoelectric literature are based on a direct melting method starting from pure constituent elements.<sup>14,15,17</sup> The pure element are sealed in

\* Author to whom correspondence should be addressed.

evacuated quartz tube under high vacuum conditions (up to  $10^{-6}$  Torr) and high temperature (up to 973 K). Moreover, the synthesis methods are characterized by long time (up to 2–3 week). An et al.<sup>18</sup> developed a very simple, potentially low cost and large scale synthesis procedure by using wet chemistry method into a Teflon-lined autoclave. In particular, the synthesis time was only of 14–20 hours and the temperature was at 155 °C. This route was not employed in thermoelectric literature up to now and only undoped tetrahedrites were synthesized in the cited work. For this reason in this work was employed the method proposed by An et al. to produce undoped and Zn and Ni substituted tetrahedrites with the aim to reduce the synthesis temperature and time compared to the commonly used methods. The development of a fast and simple method of tetrahedrites for thermoelectric application is very important to reduce the production cost of this material allowing a large scale diffusion of thermoelectric technology. Moreover, the role Zn and Ni introduction ( $\text{Cu}_{10}\text{NiZnSb}_4\text{S}_{13}$ ) in pure tetrahedrite was investigated. Open die pressing sintering (ODP) was chosen as the sintering methods to obtain fully dense materials. In fact, the powders obtained by solvothermal synthesis are characterized by nanometric size and the ODP process permit to obtain nanostructured sintered material. This point is very important in thermoelectric field, because many recent studies showed that nanostructures provide a chance to disconnect the linkage between thermal and electrical transport by introducing some new scattering mechanisms. Nanostructural design seem to be an effective way to reduce the lattice thermal conductivity increasing the ZT of the materials.<sup>19,20</sup> The ODP conditions were selected on the basis of previous work where various parameters (temperature, pressure, and time) were investigated for a wide range of materials.<sup>21,22</sup>

## 2. EXPERIMENTAL DETAILS

Tetrahedrite based powders were produced starting from commercial CuCl (Sigma Aldrich,  $\geq 99.995\%$ ),  $\text{SbCl}_3$  (Sigma Aldrich,  $\geq 99.99\%$ ),  $\text{ZnCl}_2$  (Sigma Aldrich, 99.999%),  $\text{NiCl}_2$  (Alfa Aesar 99%) and Tiourea ( $\text{NH}_2\text{CSNH}_2$ , Sigma Aldrich,  $\geq 99\%$ ) powders. Ethanol was employed as dispersion medium. Chlorides, Tiourea and Ethanol were added into a Teflon-lined autoclave in a glove box under Ar atmosphere. Then, the autoclave was sealed and heated at different temperature (155–200 °C) for 7-12-14-16-20 hours, to evaluate the effect of temperature, pressure and time on the tetrahedrite formation. The autoclave was naturally cooled at room temperature and the resulting powders were washed several time with water, ethanol and exane and then dried in vacuum at 50 °C for 4 hours.

The powders, manipulated in argon atmosphere, were put into an iron tube closed with aluminum plugs, designed to allow gas expulsion during the processing promoting higher densification, and ODP processed. In order to avoid

chemical reactions between Fe and the thermoelectric phase, a layer of BN was deposited on the internal surface of the tube. The processing was performed at 470 °C for 5 minutes after a pre-heating in static furnace. All the processing was performed in air, being the material protected by the external sheath.

The crystalline phases were revealed by X-ray diffraction (XRD) using a Philips PW 3710 X-Ray diffractometer with Bragg-Brentano geometry and a  $\text{CuK}\alpha$  source (40 kV, 30 mA). 2 Theta range was 5°–70 °C, with 0.02 step and a time for step between 5 sec and 8 sec. The Rietveld refinement on the XRD profiles has been exploited to obtain information about phase amounts, crystallite sizes and lattice parameters.<sup>23</sup> Simultaneous thermogravimetric and differential scanning calorimetry analysis (TG-DSC) were carried out on washed powders by means of SDT Q 600 Apparatus (TA Instrument) at 600 °C under synthetic nitrogen flow (rate 100 ml/min). The heating rate was of 5 °C/min. The sample size was 10 mg in alumina crucible. A residual gas analysis (RGA) of gas evolved during TG-DSC were analyzed by HPR20 QIC quadrupole gas analysis system, equipped with SEM detector. Data collection were carried out with MASSoft software analysis with Multiple Ion Detection.

The morphological and compositional characterizations were performed by Sigma Zeiss Field Emission Secondary Electron Microscope (FE-SEM) equipped with a Energy Dispersion Spectroscopy system (EDS- Oxford X-Max).

## 3. RESULTS

Pure tetrahedrite  $\text{Cu}_{12}\text{Sb}_4\text{S}_{13}$ , according to An et al.,<sup>18</sup> was firstly synthesized by using a chlorides 10% excess at 155 °C for 20 hours. The maximum internal pressure reached was 10 bar. After the heat treatment the autoclave was cooled at room temperature naturally (about 4 hours). The synthesis products were a black powder associated with a white fluff. The powder was separated from the fluff and then washed several time with distilled water, ethanol

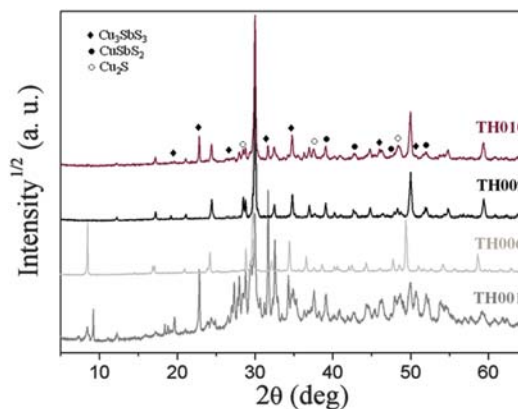
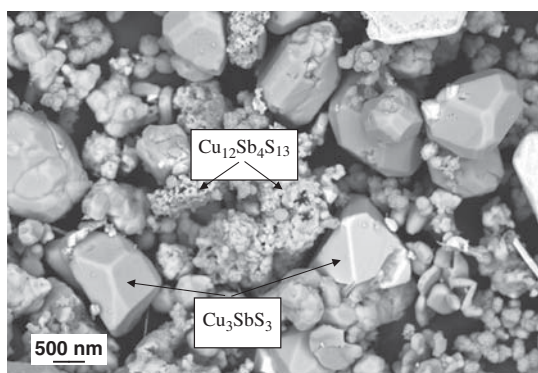


Figure 1. X-ray diffraction patterns for the tetrahedrite based powders.



**Figure 2.** FE-SEM micrograph (secondary electrons) of sample TH006.

and exane by means of a spin cycle at 7000 rpm for 15 minutes. After drying, the final product was obtained. Figure 1 shows the XRD patterns of this dried powders (TH001). The Rietveld refinement of XRD data<sup>23</sup> revealed that the tetrahedrite phase obtained was only 54 wt%, with  $\text{CuSbS}_2$  (12 wt%) and  $\text{Cu}_3\text{SbS}_3$  (orthorhombic, 34 wt%) as secondary phases.

In order to avoid the fluff formation, the synthesis temperature was increased up to 200 °C, with constant precursor quantities and time. The maximum internal pressure was 50 bar. Figure 1 (TH006) shows the XRD pattern of the obtained powders. The Rietveld refinement showed a little tetrahedrite phase increasing (up to 60 wt%), but the white fluff presence was still observed. Then the synthesis time was reduced and two new synthesis were performed at 7 hours (TH009) and 14 hours (TH010). In both cases, the fluff disappears and the Rietveld refinements showed similar tetrahedrite phase content for synthesis time of 7 hours (49 wt%) and lower for 14 hours (33 wt%) with respect to 20 hours synthesis time. As an example, Figure 2 reports the FE-SEM image of the sample TH006 showing the typical morphology of the powders. EDS analyses could not evidence the difference between

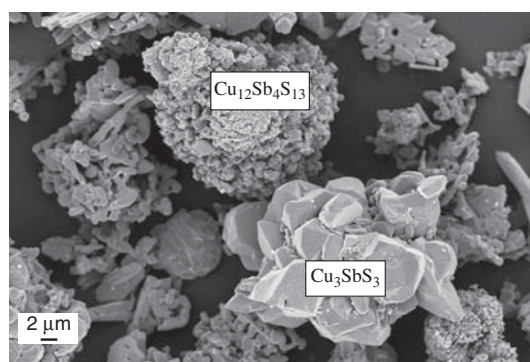


**Figure 4.** FE-SEM micrograph (secondary electrons) of sample TH013.

the two major phases,  $\text{Cu}_{12}\text{Sb}_4\text{S}_{13}$  and  $\text{Cu}_3\text{SbS}_3$ , due to the very similar composition. These two phases can be recognized by the crystal shape. Indeed, orthorhombic  $\text{Cu}_3\text{SbS}_3$  was easily identified by SEM. This phase was mainly present as micrometric crystals, whilst  $\text{Cu}_{12}\text{Sb}_4\text{S}_{13}$  phase was present as aggregate grains with nanometric size.

In order to increase the tetrahedrite phase content, the second step of this work was to change the stoichiometric ratio of the precursor in respect to An et al.<sup>18</sup> The relative amount of chlorides was not increased of 10% but the correct stoichiometric ratios were used.

The temperature was fixed at 200 °C for all synthesis, the time was 12 hours (TH013), 16 hours (TH012) and 20 hours (TH014). The Rietveld refinement of XRD data (Fig. 3)<sup>23</sup> revealed that the tetrahedrite phase obtained was 72 wt% after 12 hours of synthesis, 51 wt% after 16 hours of synthesis, and 65 wt% after 20 hours of synthesis. The revealed secondary phases were  $\text{CuSbS}_2$  (about 12 wt%),  $\text{Cu}_3\text{SbS}_3$  (orthorhombic, from 20 wt% to 34 wt%) and  $\text{Cu}_2\text{S}$  (from 15 wt% to 30 wt%). After 20 hours of synthesis the fluff was still present, whilst the synthesis performed for 12 and 16 hours did not show its presence. In order to increase the tetrahedrite phase content, 10 bar of He overpressure was inserted in the autoclave. In fact,

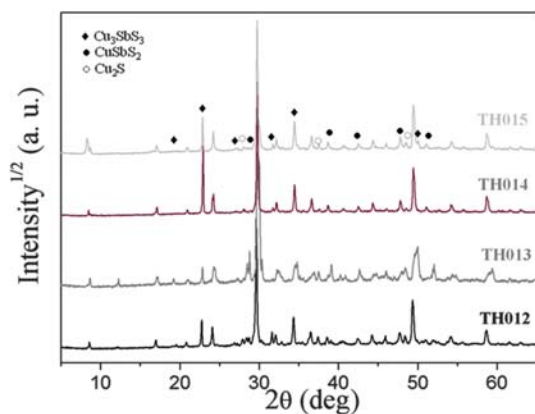


**Figure 3.** X-ray diffraction patterns for the tetrahedrite based powders obtained with the new synthesis procedure.

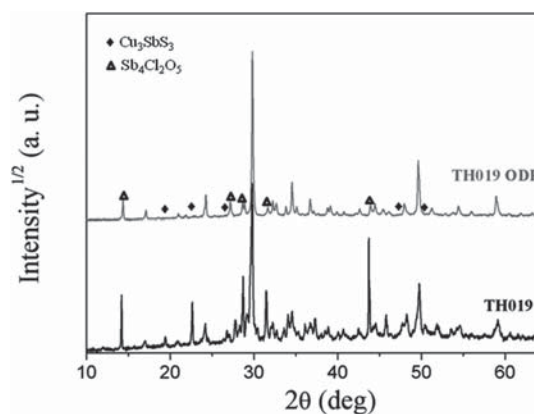


**Figure 5.** X-ray diffraction patterns for the Zn–Ni substituted tetrahedrite powders before and after ODP.



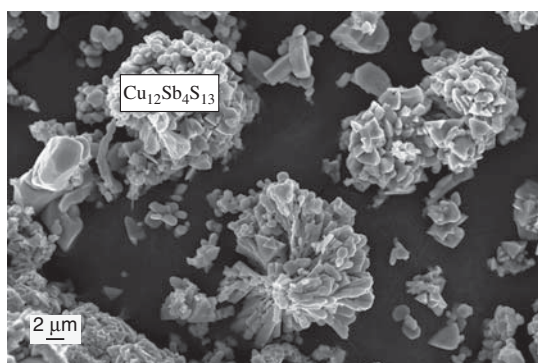
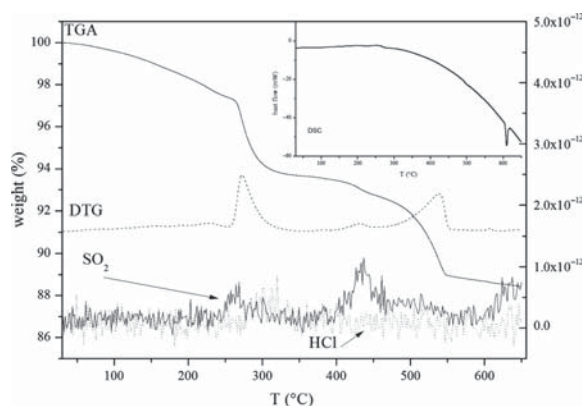
**Table 1.** List of samples studied in this work.

Sample	Time (hours)	Temperature (°C)	Notes
TH001	20	155	Literature stoichiometric ratios
TH006	20	200	Literature stoichiometric ratios
TH009	14	200	Literature stoichiometric ratios
TH010	7	200	Literature stoichiometric ratios
TH012	16	200	New stoichiometric ratios
TH013	12	200	New stoichiometric ratios
TH014	20	200	New stoichiometric ratios
TH015	20	200	New stoichiometric ratios and He overpressure
TH019	20	200	Zn and Ni doping

after 20 hours of synthesis (TH015), the tetrahedrite phase content is 78 wt% (with  $\text{Cu}_3\text{SbS}_3$  as secondary phase). These results demonstrated that working in inert gas overpressure seems to increase the tetrahedrite phase content.

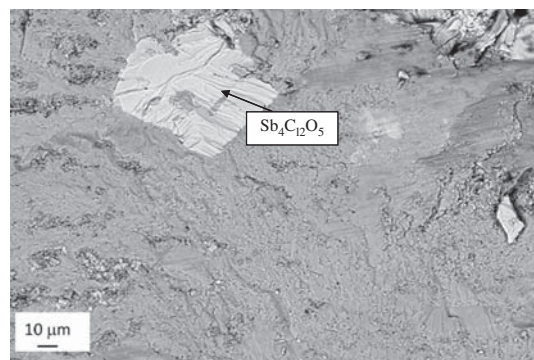
SEM images showed that the powder presented a similar shape compared with the powders obtained working with the literature conditions. In fact the tetrahedrite particles were characterized by coalescent nanometric grains, whilst the  $\text{Cu}_3\text{SbS}_3$  secondary phase was present as micrometric crystals (Fig. 4).

In order to evaluate the effect of dopant content on tetrahedrite formation in the developed synthesis procedure, Zn and Ni were added as  $\text{ZnCl}_2$  and  $\text{NiCl}_2$  with the aim to obtain the stoichiometry  $\text{Cu}_{10}\text{ZnNiSb}_4\text{S}_{13}$ . The synthesis time was 20 hours (TH019) with a fixed temperature of 200 °C. The XRD results (Fig. 5) showed that the powder were composed by tetrahedrite (43 wt%),  $\text{Cu}_3\text{SbS}_3$  (37 wt%),  $\text{CuSbS}_2$  (11 wt%) and  $\text{Sb}_4\text{Cl}_2\text{O}_5$  (9 wt%). Zn and Ni byproducts were not observed suggesting that dopant elements were successful introduced into the tetrahedrite structure. Since the Antimony Pentoxide Dichloride (hereinafter ADP) was not previously observed as secondary phase in the pure tetrahedrite synthesis, probably it could arise as a consequence of the dopant elements introduction. FE-SEM images of the powder (Fig. 6) confirmed the morphology yet observed for all phases in the other samples studied in this work. All samples with

**Figure 6.** FE-SEM micrograph (secondary electrons) of sample TH019.**Figure 7.** Thermogravimetric analysis on tetrahedrite based powders.

respective temperature and synthesis time are reported in Table I.

A thermogravimetric study was carried out on the powders with the aim of detect eventual decomposition reactions or phase transitions (Fig. 7). The TGA curve showed a weight loss of about 12% up to 600 °C in Nitrogen flow. In particular from DTG were observed two main peaks in the range of 250 °C to 310 °C and 450 °C to 550 °C. By means of RGA analyses peaks can be attributed to  $\text{SO}_2$  and  $\text{HCl}$  formation (Fig. 7). According to DSC curve a phase transition was detected at about 600 °C (Fig. 7 inset). For this reason the consolidation of these powders were carried out via Open Die Pressing at lower temperature (470 °C). The Rietveld refinement of XRD pattern of the sintered pellet showed that the sample was composed of tetrahedrite (81 wt%) and APD (19 wt%).  $\text{Cu}_3\text{SbS}_3$  and  $\text{CuSbS}_2$  secondary phases during the ODP process were totally converted. These result showed that the ODP consolidation can increase the total tetrahedrite content. In light of this experimental evidence further dopant concentration will be investigated even if, after the synthesis step, the single tetrahedrite phase formation will not occurred completely. Moreover, the consolidated sample showed a relative density of 98.5%. This high density was

**Figure 8.** FE-SEM micrograph (backscattered electrons) of sample TH019 after ODP consolidation.

confirmed by SEM analyses (Fig. 8), where, collecting the backscattered electrons highlighted the presence of the two constituent phases.

#### 4. CONCLUSION

In this work a new solvothermal synthesis method to obtain pure and Zn and Ni substituted tetrahedrite was developed. With this procedure nanometric tetrahedrite particles were obtained, associated with secondary phases with micrometric size. Preliminary consolidation test were carried out on Zn and Ni doped powders. During the ODP sintering process most of these secondary phases disappeared and the total content of tetrahedrite increased from 48 wt% to 81 wt%.

In light of this experimental evidence further dopant concentration should be investigated even if after the synthesis step a single tetrahedrite phase will not occurred.

The synthesis time was significantly reduced in respect to literature and the total time to obtain tetrahedrite based powders was at least 12 hours in autoclave and 4 hours to evaporate the solvent.

**Acknowledgments:** The authors are grateful to Dr. Agresti for the inestimable help for the Rietveld refinements and to Mr. Enrico Bassani for the ODP processing. This work has been funded by the Italian National Research Council—Italian Ministry of Economic Development Agreement “Ricerca di sistema elettrico nazionale.”

#### References and Notes

1. J. W. Miller and J. R. Craig, *Amer. Mineral.* 68, 227 (1983).
2. A. A. Godonikov and N. A. Il'yasheva, *Int. Geol. Rev.* 15, 1413 (1973).
3. N. E. Johnson, J. R. Craig, and J. D. Rimstidt, *Can. Mineral.* 24, 385 (1986).
4. J. T. Nash, *Econ. Geol.* 68, 34 (1973).
5. I. Wu and U. Petersen, *Econ. Geol.* 72, 99 (1977).
6. H. Catchpole, K. Kouzmanov, B. Putlitz, J. H. Seo, and L. Fontboté, *Econ. Geol.* 110, 39 (2015).
7. J. W. Anthony, R. A. Bideaux, K. W. Bladh, and K. W. Nichols, *Mineral. Soc. Amer.* 1, 20151 (2003).
8. A. Buzatu, G. Damian, H. G. Dill, N. Buzgar, and A. I. Apopei, *Ore Geol. Rev.* 65, 132 (2015).
9. R. D. Vassileva, R. Atanassova, and K. Kouzmanov, *Mineral. Petrol.* 1, 17 (2013).
10. T. Wagner and E. Jonsson, *Can Mineral.* 39, 855 (2001).
11. S. Fadda, M. Fiori, and S. M. Grillo, *Geochem. Mineral. Petrol.* 43, 79 (2005).
12. F. Minz, N.-J. Bolin, P. Lamberg, and C. Wanhainen, *Miner. Eng.* 52, 95 (2013).
13. V. Atanasov, *Mineral. Mag.* 40, 233 (1975).
14. X. Lu, D. T. Morelli, Y. Xia, F. Zhou, V. Ozolins, H. Chi, X. Zhou, and C. Uher, *Advanced Energy Materials* 3, 342 (2013).
15. K. Suekuni, K. Tsuruta, M. Kunii, H. Nishiate, E. Nishibori, S. Maki, M. Ohta, A. Yamamoto, and M. Koyano, *J. Appl. Phys.* 113, 043712 (2013).
16. X. Lu, D. T. Morelli, Y. Xia, and V. Ozolins, *Chem. Mat.* 27, 408 (2015).
17. R. Chetty, P. K. D. S, G. Rogl, P. Rogl, E. Bauer, H. Michor, S. Suwas, S. Puchegger, G. Giester, and R. C. Mallik, *Phys. Chem. Chem. Phys.* 17, 1716 (2015).
18. C. An, Y. Jin, K. Tang, and Y. Qian, *J. Mat. Chem.* 13, 301 (2003).
19. J.-F. Li, W.-S. Liu, L.-D. Zhao, and M. Zhou, *NPG Asia Mater.* 2, 152 (2010).
20. Z.-G. Chen, G. Han, L. Yang, L. Cheng, and J. Zou, *Progr. Nat. Sci.: Mater. Int.* 22, 535 (2012).
21. S. Ceresara, C. Fanciulli, F. Passaretti, and D. Vasilevskiy, *J. Electron. Mater.* 42, 1529 (2013).
22. C. Fanciulli, S. Battiston, S. Boldrini, E. Villa, A. Famengo, S. Fiameni, M. Fabrizio, and F. Passaretti, *Mater Today: Proc.* 2, 566 (2015).
23. L. Lutterotti, S. Matthies, H. R. Wenk, A. S. Schultz, and J. W. Richardson Jr., *J. Appl. Phys.* 81, 594 (1997).

Received: 22 March 2016. Accepted: 24 May 2016.